IEICE TRANS. ELECTRON., VOL.E82–C, NO.11 NOVEMBER 1999

PAPER

A Compact Smith-Purcell Free-Electron Laser with a Bragg Cavity

Tipyada THUMVONGSKUL[†a)], ***Nonmember***, **Akimasa HIRATA**[†], ***Student Member***, ***and*** **Toshiyuki SHIOZAWA**[†], ***Member***

SUMMARY The growth and saturation characteristics of an electromagnetic (EM) wave in a Smith-Purcell free-electron laser (FEL) with a Bragg cavity are investigated in detail with the aid of numerical simulation based upon the fluid model of the electron beam. To analyze the problem, a two-dimensional (2-D) model of the Smith-Purcell FEL is considered. The model consists of a planar relativistic electron beam and a parallel plate metallic waveguide, which has a uniform grating carved on one plate. For confinement and extraction of EM waves, a Bragg cavity is formed by a couple of reflector gratings with proper spatial period and length, which are connected at both ends of the waveguide. The results of numerical simulation show that a compact Smith-Purcell FEL can be realized by using a Bragg cavity composed of metallic gratings.

key words: *Bragg cavity, compact lasers, high-power lasers, metallic gratings, Smith-Purcell FEL*

1. Introduction

One of the major topics in recent research of FEL's is to realize compact FEL's [1]–[3], which are desirable for various applications such as space communications, high-resolution radars, remote sensing, laser surgeries, and so forth. In the previous work [4], it was shown that a compact Cherenkov laser can be realized by using a Bragg cavity composed of dielectric gratings. For one of the problems encountered in the Cherenkov laser, however, it has been known that the slow wave structure composed of a dielectric-loaded waveguide can cause dielectric breakdown by being exposed to high intensities of electric field. In addition, for proper operation, special attention must be paid to drain off electric charges accumulated on the dielectric surface. To avoid the problems stated above, we propose in this paper a compact Smith-Purcell FEL with a Bragg cavity, which uses metallic gratings, instead of dielectrics, for the slow wave structure. In recent years, it has been reported that high-power radiation can be generated at millimeter or submillimeter wavelengths in Smith-Purcell FEL's [5]–[10].

For the proposed model of a Smith-Purcell FEL with a Bragg cavity, the growth and saturation characteristics of the EM wave are investigated in detail with the aid of numerical simulation based upon the fluid model of the electron beam. To analyze the problem, a 2-D model of the Smith-Purcell FEL is considered. The 2-D model consists of a planar relativistic electron beam and a parallel plate waveguide, on one plate of which a uniform grating is carved, and at both ends of which a couple of reflector gratings with proper spatial period and length are connected to form a Bragg cavity.

To prepare for the numerical simulation, we first show in Sect. 2 the dispersion relation for the coupled EM and space-charge waves propagated along a planar relativistic electron beam drifting in a parallel plate waveguide with a uniform metallic grating. From this dispersion relation, we obtain the spatial growth rate for the growing EM waves at a specified frequency. Next, in Sect. 3, we give the power reflection and transmission coefficients for metallic gratings which form a Bragg cavity. In Sect. 4, by following the same procedure as used in the previous work [4], taking into account the decrease in the drift velocity of the electron beam based on the energy conservation law, we numerically calculate the growing power extracted from the Bragg cavity. From the numerical analysis, we find that a compact Smith-Purcell FEL can be realized by using a Bragg cavity composed of metallic gratings. A brief conclusion is given in Sect. 5.

2. Dispersion Relation for Coupled Waves

The geometry of the problem is shown in Fig. 1, together with the coordinate system. The 2-D Smith-Purcell FEL considered in this paper consists of a parallel plate waveguide, which has gratings carved on the

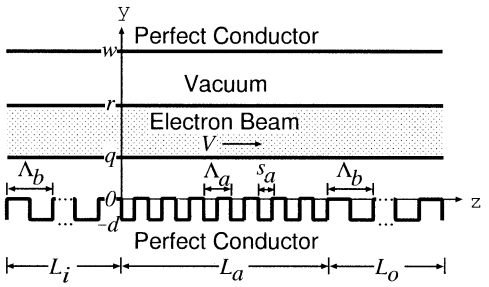

Fig. 1 Geometry of the problem.

Manuscript received December 2, 1998.
Manuscript revised May 11, 1999.

[†]The authors are with the Department of Communication Engineering, Graduate School of Engineering, Osaka University, Suita-shi, 565-0871 Japan.
a) E-mail: tipyada@comm.eng.osaka-u.ac.jp

surface of the lower conducting plate, and a planar relativistic electron beam drifting with velocity V through it. The separation between two conducting plates is w, the thickness of a planar electron beam $r-q$, and the beam-grating gap q. In the interaction region, the grating carved on the lower conducting plate has the period Λ_a, the slot width s_a equal to $\Lambda_a/2$, and the groove depth d. At both ends of the interaction region, a couple of reflector gratings with the proper period Λ_b, which approximately satisfies the Bragg condition over a certain frequency range around the operating point, are connected to form a Bragg cavity. The reflector gratings are separated from each other by the distance L_a. The lengths of the reflector gratings, L_i and L_o are adjusted to gain the required reflection and transmission coefficients. For simplicity, the electron beam is assumed to be ion-neutralized, with no magnetostatic field applied on it.

Let us consider the coupling between a negative-energy space-charge wave propagated along a relativistic electron beam and a slow EM wave propagated along a parallel plate waveguide, which has a uniform grating carved on the lower conducting plate. The basic equations for the analysis are the Maxwell equations, the relativistic equation of motion for the electron, and the equation of continuity for the electron flow [11]. On the assumption that the slot width s_a is much smaller than the wavelength in free space, the fields in the slot can be approximately expressed in terms of TEM standing waves. On the other hand, the fields over the metallic gratings (both in the vacuum and beam regions) can be represented in terms of spatial harmonics [12] with axial wave numbers k_n given by

$$k_n = k_z + \frac{2n\pi}{\Lambda_a} \quad (n = 0, \pm 1, \pm 2, ...) \tag{1}$$

k_z being the wave number for the coupled wave of the zeroth order spatial harmonic in the z direction.

By imposing the boundary conditions at the surfaces of the electron beam [11], the metallic grating [12], and the conducting plate on the field components obtained above, we have the following dispersion relation for the coupled EM and space-charge waves of the TM mode [10], [13]:

$$1 - \frac{\omega s_a}{\mathrm{c}} \tan\left(\frac{\omega d}{\mathrm{c}}\right) \sum_{n=-\infty}^{\infty} \frac{\Phi_n}{h_{yn}\Lambda_a \Psi_n} \mathrm{sinc}^2\left(\frac{k_n s_n}{2}\right) = 0 \tag{2}$$

with

$$\begin{aligned}
\Phi_n = {} & (k_{yn} \tanh h_{yn} q \ \ \tanh k_{yn} q - \varepsilon_{pn} h_{yn}) \\
& \cdot(\varepsilon_{pn} h_{yn} \tanh k_{yn} r \ \ \tanh h_{yn}(w-r) + k_{yn}) \\
& -(k_{yn} \tanh h_{yn} q - \varepsilon_{pn} h_{yn} \tanh k_{yn} q) \\
& \cdot(\varepsilon_{pn} h_{yn} \tanh h_{yn}(w-r) + k_{yn} \tanh k_{yn} r) \\
\Psi_n = {} & (k_{yn} \tanh k_{yn} q - \varepsilon_{pn} h_{yn} \tanh h_{yn} q) \\
& \cdot(\varepsilon_{pn} h_{yn} \tanh k_{yn} r \ \ \tanh h_{yn}(w-r) + k_{yn}) \\
& -(k_{yn} - \varepsilon_{pn} h_{yn} \tanh h_{yn} q \ \ \tanh k_{yn} q) \\
& \cdot(\varepsilon_{pn} h_{yn} \tanh h_{yn}(w-r) + k_{yn} \tanh k_{yn} r)
\end{aligned}$$

$$\mathrm{sinc}\left(\frac{k_n s_n}{2}\right) = \sin\left(\frac{k_n s_n}{2}\right) \Big/ \left(\frac{k_n s_n}{2}\right)$$

$$h_{yn}^2 = k_n^2 - \left(\frac{\omega}{\mathrm{c}}\right)^2$$

$$k_{yn}^2 = k_n^2 + \left(\frac{\omega_p}{\mathrm{c}}\right)^2 - \left(\frac{\omega}{\mathrm{c}}\right)^2$$

$$\varepsilon_{pn} = 1 - \left(\frac{\omega_p}{\gamma s_n}\right)^2$$

$$s_n = \omega - k_n V$$

$$\gamma = \frac{1}{\sqrt{1-\beta^2}}$$

$$\beta = \frac{V}{\mathrm{c}} \tag{3}$$

where ω and c denote the angular frequency and the speed of light in vacuum, ω_p, β and γ being the angular plasma frequency, the relative drift velocity and the relativistic factor of the electron beam. The symbols h_{yn} and k_{yn} are the transverse wave numbers corresponding to the nth spatial harmonic in vacuum and beam regions, respectively. In a particular range of frequencies, the dispersion relation (2) has two complex roots for k_z which are complex conjugate to each other, corresponding to growing and decaying waves. The decaying wave decays rapidly within a few wavelengths, while the growing one grows exponentially along the propagating direction z by the spatial growth rate α (the imaginary part of k_z for the growing wave). The coupling between the EM wave and the electron beam is incorporated in the spatial growth rate. By numerically solving the dispersion relation (2), we can find the spatial growth rate and the longitudinal wave number for the growing wave in that particular range of frequencies.

Instead of directly solving (2), however, we can roughly find the relation between the operating frequency and the longitudinal wave number for the coupled wave in a more simplified manner. First, in the absence of the electron beam ($\omega_p = 0$), the dispersion relation for the TM polarized EM wave propagated in a metallic grating waveguide reads

$$1 - \frac{\omega s_a}{\mathrm{c}} \tan\left(\frac{\omega d}{\mathrm{c}}\right) \cdot \sum_{n=-\infty}^{\infty} \frac{1}{h_{yn}\Lambda_a \tanh(h_{yn} w)} \mathrm{sinc}^2\left(\frac{k_n s_n}{2}\right)$$

$$= 0. \tag{4}$$

On the other hand, the dispersion relation for the space-charge wave propagated along a relativistic electron beam in a smooth waveguide with no metallic gratings takes a simplified form $\omega - k_z V = \pm\omega_p/\sqrt{2}\gamma$, which can be approximated, for the case $\omega_p \ll \omega$, as

$$k_z = \frac{\omega}{V}. \tag{5}$$

We find that the operating point (ω, k_z) is located around the intersection of the dispersion curves (4) and (5) on the dispersion diagram. This approximate operating point is helpful as a starting point in numerically solving (2) for the actual values of the spatial growth rate and the longitudinal wave number. The concept of energy conservation provides us a systematic scheme to follow the growth of the EM wave and the decrease in the kinetic energy of the electron beam along the coupling process. The numerical results are discussed in Sect. 4.

3. Reflection and Transmission Coefficients of a Metallic Grating

As shown in Fig. 2, a section of a metallic grating waveguide is considered. In our analysis of the Smith-Purcell FEL with a Bragg cavity, we need to know the power reflection and transmission coefficients at $z = 0$ and $z = l$. In the section of a metallic grating waveguide illustrated in Fig. 2, we consider the coupling for the forward and backward dominant TM modes. Let B^+ and B^- be the amplitudes of the forward and backward dominant modes, respectively, which are slowly varying in the z direction. Then, solving the coupled-mode equations relating B^+ and B^- under the assumptions $B^+(0) = B(0)$ at $z = 0$, and $B^-(l) = 0$ at $z = l$, we find [1], [14], [15] that

$$\begin{aligned} B^-(z) &= B(0)\cdot\{\mathrm{j}\kappa e^{-\mathrm{j}\Delta k_z z}\sinh[S(z-l)]\}/ \\ &\quad \{-\Delta k_z \sinh(Sl) + \mathrm{j}S\cosh(Sl)\} \\ B^+(z) &= B(0)\cdot\{e^{+\mathrm{j}\Delta k_z z}\{\Delta k_z \sinh[S(z-l)] \\ &\quad +\mathrm{j}S\cosh[S(z-l)]\}\}/ \\ &\quad \{-\Delta k_z \sinh(Sl) + \mathrm{j}S\cosh(Sl)\} \end{aligned} \tag{6}$$

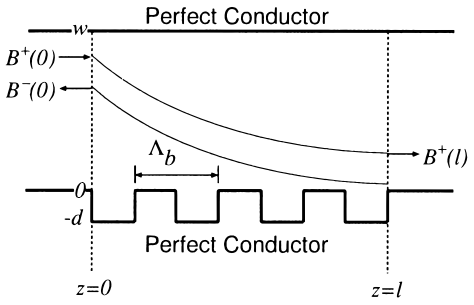

Fig. 2 Reflection and transmission by a metallic grating.

with

$$\kappa = \mathrm{j}\frac{d}{\pi w}\frac{(\omega/\mathrm{c})^2 + k_z^2}{k_z}$$

$$\Delta k_z = k_z - \pi/\Lambda_b$$

$$S = \sqrt{|\kappa|^2 - (\Delta k_z)^2} \tag{7}$$

where $B(0)$ is the initial amplitude of the forward wave entering the metallic grating at $z = 0$, κ is the coupling coefficient between the forward and backward dominant modes, and Δk_z denotes the phase constant mismatch from the Bragg condition.

From (6), we can define the power reflection coefficient at $z = 0, R$ and the power transmission coefficient at $z = l, T$ as

$$\begin{aligned} R &= \left|\frac{B^-(0)}{B(0)}\right|^2 \\ T &= \left|\frac{B^+(l)}{B(0)}\right|^2, \end{aligned} \tag{8}$$

respectively. From the above equations, we find that the reflection coefficient has its peak value when the Bragg condition $\Delta k_z = 0$ is satisfied.

4. Growth and Saturation Characteristics

In the Smith-Purcell FEL considered in this paper, growing waves are generated through the active coupling of an EM wave (positive-energy wave) propagated along a metallic grating waveguide and a slow space-charge wave (negative-energy wave) propagated along a relativistic electron beam. In other words, the growth of the EM wave is compensated for by the growth of the negative-energy space-charge wave, corresponding to the decrease in the kinetic energy of the electron beam. Thus, the kinetic energy of the electron beam is transferred to the EM wave through the coupling of the latter with the negative-energy space-charge wave.

At the time $t = 0$, let us inject a single EM wave packet or pulse of fixed center frequency ω and longitudinal length L, which is assumed, for simplicity, to be shorter than $2L_a$ but much longer than the guide wavelength $\lambda_g (= 2\pi/k_z)$, at the entrance of the Bragg cavity, $z = 0$ in Fig. 1. Then, according to the prescription of energy conservation and the corresponding numerical treatment described in the previous work [4], we numerically follow step by step the gradual growth and saturation of the EM wave packet which gains energy from the electron beam while traveling back and forth between the two metallic-grating mirrors. At the same time, we also investigate how the EM wave packet extracted from the Bragg cavity reaches a steady state. In each transit, the EM wave makes one round trip between the two metallic-grating mirrors, taking the time

Table 1 Values of parameters used in numerical simulation.

Waveguide and Bragg Cavity	
Separation between Conducting Plates w	3.6 [mm]
Groove Depth of Grating d	0.36 [mm]
Spatial Period of Grating Λ_a	0.36 [mm]
Separation between Grating Mirrors L_a	12 [cm]
Spatial Period of Reflector Grating Λ_b	0.96 [mm]
Length of Reflector Grating 1 L_i	1.2 [cm]
Length of Reflector Grating 2 L_o	0.5 [cm]
Electron Beam	
Beam Thickness $(r-q)$	0.36 [mm]
Beam-Grating Gap q	0.36 [mm]
Electron Density N	4.93×10^9 [/cm^3]
Initial Normalized Drift Velocity V_0/c	0.82
Plasma Frequency $\omega_p/2\pi$	477 [MHz]
Initial Beam Voltage	382 [kV]
Initial Beam Current	0.7 [A/cm]
EM Wave	
Frequency $\omega/2\pi$	121 [GHz]
Guide wavelength λ_g	2.02 [mm]
Initial EM Power	10 [μW/cm]

approximately equal to $t_1 = 2L_a/V_0$. In the operation regime considered in this paper, the EM wave traveling in the forward direction interacts actively with the electron beam and exponentially grows, gaining energy from the latter. On the other hand, there is no net energy transfer from the electron beam to the EM wave traveling in the backward direction. If we assume that both the electron beam and the parallel plate waveguide in Fig. 1 are nondissipative, then the EM wave travels in the backward direction in the Bragg cavity, retaining the average power. The time that the EM wave reaches its saturation can be approximately calculated from $t_n = (2n-1)L_a/V_0$, where n is the number of transit for the EM wave to reach its saturation. Thus, if we wish to have a steady EM pulse extracted from the Bragg cavity, the relativistic electron beam should persist for a period of time longer than the saturation time t_n.

The values of parameters used in the numerical simulation are listed in Table 1. The initial drift velocity of the electron beam and the frequency of the EM wave are appropriately chosen so that the velocity matching between them can be satisfied. The operating frequency picked out in the above manner is 121 GHz, which corresponds to the guide wavelength of 2.02 mm. In addition, we chose the length of the reflector grating at the output side of the Bragg cavity in such a way that the EM power extracted from it becomes maximum with the other parameters fixed.

First, we show in Fig. 3 the temporal variation of the spatial growth rate for the growing wave α. As seen from Fig. 3, the spatial growth rate gradually decreases as the beam-wave interaction progresses, and it finally reduces to zero at the end of the Bragg cavity. At the initial stage of the interaction, when the level of the EM power is very low, the spatial growth rate varies only slightly. However, as the EM wave grows and gradually

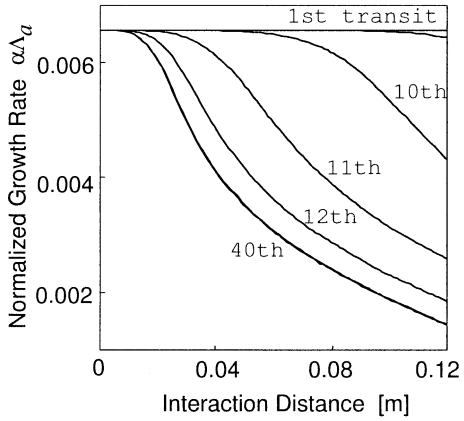

Fig. 3 Temporal variation of the spatial growth rate.

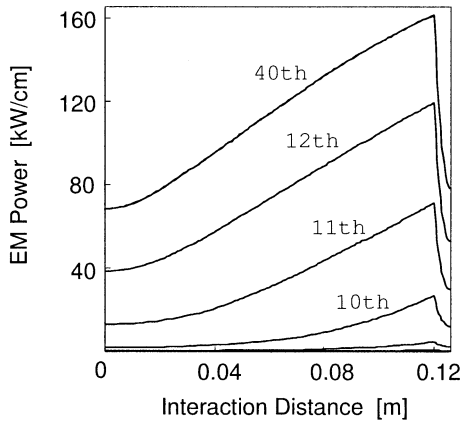

Fig. 4 Temporal growth of the EM power in the Bragg cavity.

gets out of synchronism with the electron beam, which has its drift velocity decreasing along the process, it decreases more and more rapidly from transit to transit. At the end of the Bragg cavity, when the spatial growth rate drops down to zero, the EM wave stops growing and the extracted EM power gets saturated.

Figure 4 illustrates the temporal growth of the EM power confined in, and extracted from, the Bragg cavity as the beam-wave interaction progresses. As is evident from Fig. 4, the growth of the EM wave gradually slows down and eventually gets saturated with increasing numbers of the transit between the grating mirrors. With the parameters shown in Table 1, we have about 79 kW/cm and 160 kW/cm, respectively, for the saturated values of the EM power extracted from the Bragg cavity and the intracavity EM power. The time for the EM wave to reach its 22nd transit, which is considered near the saturation time, is about 21.1 μs (with a difference from the time predicted by $t_n = (2n-1)L_a/V_0$ less than 0.5%). In the case of a single-pass Smith-Purcell FEL, the numerical results show that the EM power gets saturated at $z = 0.9$m, with the saturated value of 110 kW/cm and the consumed time 3.76 μs.

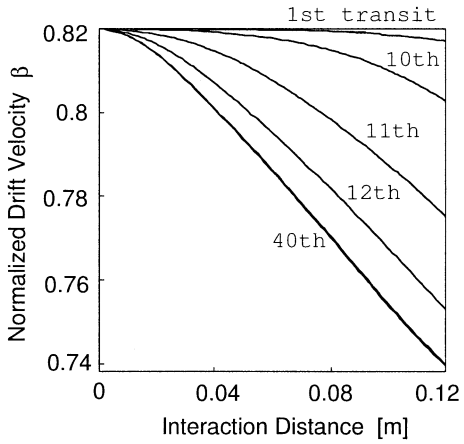

Fig. 5 Temporal variation of the drift velocity.

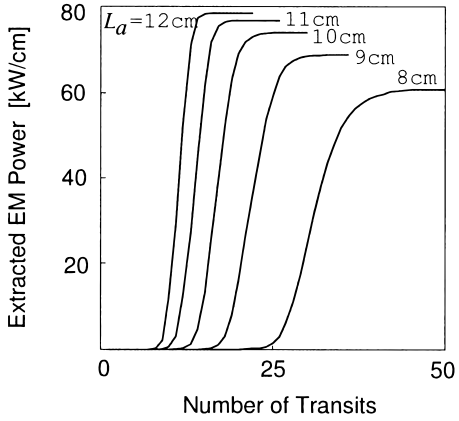

Fig. 6 Temporal growth of the EM power extracted from the Bragg cavity.

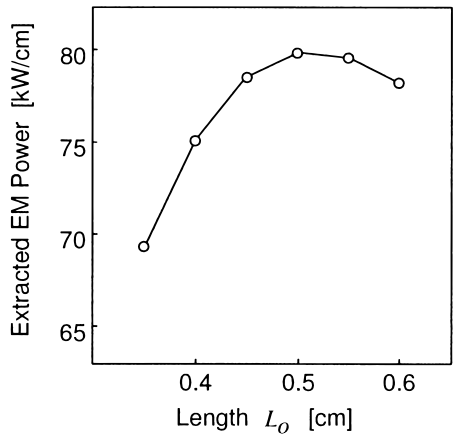

Fig. 7 EM power extracted from the Bragg cavity versus the length L_0 of the reflector grating at the output end.

The efficiency of energy transfer η can be calculated from the kinetic energy change in the relativistic electron beam, which can directly be found from its drift velocity, as

$$\eta = \frac{W_p^0 - W_p}{W_p^0}, \qquad W_p = (\gamma - 1)m_0c^2 \tag{9}$$

where W_p denotes the kinetic energy of the electron at the saturation time (m_0 is the rest mass of the electron), while W_p^0 is that at the initial stage. Figure 5 shows the temporal variation of the drift velocity of the electron beam, illustrating how the drift velocity of the electron beam gradually decreases and finally approaches a saturated value. Here, the efficiency of about 15% can be achieved in this numerical simulation, where the initial power of the electron beam is 267 kW/cm. From Figs. 4 and 5, we confirm that the growth of the EM wave is compensated for by the decrease in the kinetic energy of the electron beam.

Next, we consider how the power extracted from the Bragg cavity temporally grows for various values of the interval between the grating mirrors L_a. Figure 6 shows the relation between the EM power extracted from the Bragg cavity and the number of transits. In our numerical calculations in Fig. 6, the value of the length of the reflector grating on the output side of the Bragg cavity L_o is chosen for different values of L_a in such a way that the extracted EM power becomes maximum in each case. At the output end of our model in Fig. 1, we have a series of EM pulses separated by the period of time nearly equal to $2L_a/V_0$ while the electron beam persists if we initially inject a single EM wave packet or pulse with longitudinal length shorter than $2L_a$ at the entrance of the Bragg cavity. Note that the curves in Fig. 6 were obtained by connecting the peak values of extracted EM pulses. As seen from Fig. 6, the extracted EM power gets saturated more rapidly for the larger values of L_a, due to the higher gain per transit. However, the saturated values of the extracted EM power can no longer become so high for large values of L_a, since in this case the spatial growth rate decreases rapidly from transit to transit (see Fig. 3). On the other hand, for a more compact device (for which L_a becomes smaller), the gain per transit is pretty low, and this requires much more transits for the EM wave to reach saturation. As a matter of fact, for too short L_a, the electron beam will pass the Bragg cavity before the EM pulses can reach a steady state. Thus, we should avoid over-shortening an interval between the grating mirrors as well.

Finally, we discuss some aspects on the dimensions for the Bragg reflectors. As the length of a reflector grating becomes longer, the reflection coefficient becomes larger, too. Since there is no need to extract the EM power from the Bragg cavity at the input end, we can specify the value of L_i such that the reflection coefficient has its value close to unity. On the other hand, there is a trade-off in selecting the value of L_o. We need a large value of reflection coefficient in order to reflect the EM wave back to be further amplified, while it is also indispensable to have a sufficient value

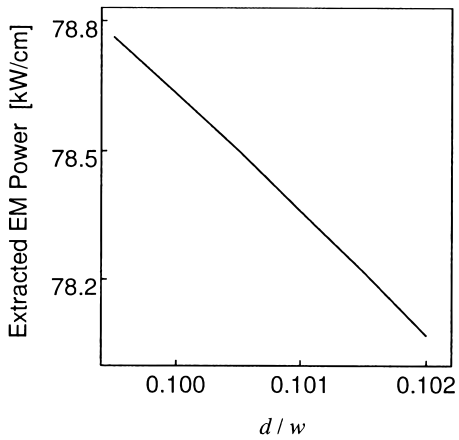

Fig. 8 EM power extracted from the Bragg cavity versus the ratio d/w of the reflector grating at the output end.

of transmission coefficient to allow a fraction of the EM power to be extracted at the output end. In the simulation, as shown in Fig. 7, we find that there is a certain value of L_o which can overcome this trade-off and gives us the maximum extracted EM power. Similarly, to see how the depth d of the reflector grating affects the output power level, we illustrate in Fig. 8 the relation between the extracted EM power and the ratio d/w of the reflector grating at the output end. The ratio d/w is one of the parameter to specify the value of κ as shown in (7), and hence its variation can be considered equivalent to changing κ. Here, the ratio d/w can be varied only in a small range in order to keep $S = \{|\kappa|^2 - (\Delta k_z)^2\}^{1/2}$ as a real number, and thus the forward and backward waves can couple in the sense shown in Fig. 2 along the reflector grating. From the discussion in Sect. 3, we know that different values of κ can affect the reflection and transmission coefficients of the EM wave at the Bragg mirror, and hence the resulted output power for the total system. However, we can conclude from Fig. 8 that the extracted EM power does not significantly depend on the parameter κ of the reflector grating, compared with changing the value of L_a or L_o (see Figs. 6 and 7).

5. Conclusion

With the aid of numerical simulation based upon the fluid model of the electron beam, we discussed the growth and saturation characteristics of the EM wave in a Smith-Purcell FEL with a Bragg cavity composed of metallic gratings. For the analysis of the problem, we considered a 2-D model of the Smith-Purcell FEL. The 2-D model consists of a planar relativistic electron beam and a parallel plate waveguide, on one plate of which a uniform grating is carved, and at both ends of which reflector gratings with proper period and length are connected to form a Bragg cavity for confinement and extraction of the EM wave. In the model specified above, we initially injected a single EM wave packet or pulse of fixed frequency and longitudinal length shorter than twice the interval between the grating mirrors, but much longer than the guide wavelength of the EM wave, at the entrance of the Bragg cavity. Then, we numerically followed step by step the beam-wave interaction process, and clarified how the EM wave packet gradually grew and finally reached a saturated level while traveling back and forth between the two metallic-grating mirrors. At the same time, we also investigated how the EM wave power extracted from the Bragg cavity reached a steady state. The results of the numerical simulation demonstrate that a compact Smith-Purcell FEL can be realized by using a Bragg cavity composed of metallic gratings.

Acknowledgement

A part of this work was supported by the grant-in-aid for Scientific Research of the Ministry of Education, Science, Sports and Culture of Japan.

References

[1] M.C. Wang, V.L. Granatstein, and R.A. Kehs, "Design of a Bragg cavity for a millimeter wave free-electron laser," Appl. Phys. Lett., vol.48, pp.817–819, 1986.
[2] E. Fisch, A.K. Henning, and J. Walsh, "A Cherenkov microlaser," IEEE J. Quantum Electron., vol.27, pp.753–759, 1991.
[3] K. Mima, S. Nakai, T. Taguchi, N. Ohigashi, Y. Tsunawaki, K. Imasaki, C. Yamanaka, and M. Shiho, "A new FEL concept driven by a vacuum microfield emitter," Nuclear Instruments and Methods in Physics Research, A331, pp.550–553, 1993.
[4] T. Shiozawa and H. Kamata, "A compact Cherenkov laser with a Bragg cavity composed of dielectric gratings," IEEE J. Quantum Electron., vol.33, pp.1687–1693, 1997.
[5] J. Walsh, T.L. Buller, B. Johnson, G. Dattoli, and F. Ciocci, "Metal-grating far-infrared free-electron lasers," IEEE J. Quantum Electron., vol.21, pp.920–923, 1985.
[6] D.E. Wortman, R.P. Leavitt, H. Dropkin, and C.A. Morrison, "Generation of millimeter-wave radiation by means of a Smith-Purcell free-electron laser," Phys. Rev., vol.24, pp.1150–1153, 1981.
[7] E.M. Marshall, P.M. Phillips, and J.E. Walsh, "Planar orotron experiments in the millimeter wavelength band," IEEE Trans. Plasma Sci., vol.16, pp.199–205, 1988.
[8] G. Doucas, J.H. Mulvey, and M. Omori, "First observation of Smith-Purcell radiation from relativistic electrons," Phys. Rev. Lett., vol.69, pp.1761–1764, 1992.
[9] J.M. Wachtel, "Free-electron lasers using the Smith-Purcell effect," J. Appl. Phys., vol.50, pp.49–56, 1979.
[10] T. Shiozawa and M. Sata, "Efficiency enhancement in a Smith-Purcell free-electron laser," Appl. Phys. Lett., vol.66, pp.124–126, 1995.
[11] T. Shiozawa and T. Nakashima, "Two-dimensional mode analysis of the Raman-type free-electron laser," J. Appl. Phys., vol.55, pp.637–646, 1984.
[12] R.E. Collin, Foundations for Microwave Engineering, McGraw-Hill Kogakusha, Ltd., Tokyo, 1966.
[13] B.D. McVey, M.A. Basten, J.H. Booske, J. Joe, and J.E. Scharer, "Analysis of rectangular waveguide-gratings

for amplifier applications," IEEE Trans. Microwave Theory Tech., vol.42, pp.995–1003, 1994.
[14] A. Yariv, "Coupled-mode theory for guided-wave optics," IEEE J. Quantum Electron., vol.9, pp.919–933, 1973.
[15] A. Yariv, Quantum Electronics, 3rd Ed., pp.606–615, John Wiley & Sons, New York, 1988.

Tipyada Thumvongskul was born in Bangkok, Thailand, on March 22, 1975. She received the B.E. degree in electrical engineering from Chulalongkorn University, Bangkok, Thailand, in 1996, and the M.E. degree in electrical communication engineering from Osaka University, Osaka, Japan, in 1999. She is now working toward the Ph.D. degree at Osaka University. Her current research field is the free-electron laser, especially on a compact structure.

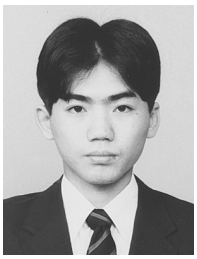

Akimasa Hirata was born in Okayama, Japan, on November 27, 1973. He received the B.E. and M.E. degrees in electrical communication engineering from Osaka University, Osaka, Japan, in 1996 and 1998, respectively. He is currently pursuing the Ph.D. degree at Osaka University. His research interests are numerical simulation on free–electron lasers and bioelectromagnetics. Mr. Hirata is a research fellow of the Japan Society for the Promotion of Science (JSPS Research Fellow).

Toshiyuki Shiozawa was born in Tokyo, Japan, on January 16, 1941. He received the B.E., M.E. and Ph.D. degrees in electrical communication engineering from Osaka University, Osaka, Japan, in 1964, 1966 and 1969, respectively. In 1969, he joined the Department of Communication Engineering, Osaka University, where he is now a Professor. He has carried out research in the area of relativistic EM theory for engineering-oriented applications, scattering of EM waves, and wave propagation in plasmas and relativistic electron beams. He has currently been engaged in research of relativistic electron beam devices for generating millimeter or submillimeter waves, such as Cherenkov, Smith-Purcell and Raman-type free-electron lasers. In 1978, he was invited to the 19th General Assembly of the International Union of Radio Science (URSI) held in Helsinki, Finland, to give a review talk on the electrodynamics of rotating systems. He has been serving as a member of Editorial Boards of the IEEE Transactions on Microwave Theory and Techniques and the Journal of Applied Physics. From 1995 to 1999, he served as an Associate Editor of the IEICE Transactions on Electronics. He is presently the Chairman of the Technical Committee on Electromagnetic Theory, IEE Japan. He is a co-author of the books *Topics in Advanced Electromagnetic Theory* (Tokyo, Japan: Corona, 1988), and *Exercise in Electromagnetic Theory* (Tokyo, Japan: Corona, 1998). Dr.Shiozawa is a member of the Institute of Electrical Engineers of Japan and a senior member of the IEEE.